On the Cooperation of Multiple Indicator-based Multi-Objective Evolutionary Algorithms

Jesús Guillermo Falcón-Cardona
Computer Science Department
CINVESTAV-IPN
Mexico City, Mexico
jfalcon@computacion.cs.cinvestav.mx

Michael T.M. Emmerich
Leiden Institute of Advanced Computer Science
Leiden University
Leiden, The Netherlands
m.t.m.emmerich@liacs.leidenuniv.nl

Carlos A. Coello Coello**
Departamento de Sistemas
UAM-Azcapotzalco
Mexico City, MEXICO
ccoello@cs.cinvestav.mx

Abstract—In recent years, several indicator-based multi-objective evolutionary algorithms (IB-MOEAs) have been proposed. Each IB-MOEA presents different search preferences depending on the quality indicator (QI) that it uses in its selection mechanism. However, due to these search biases, IB-MOEAs behave differently on each multi-objective optimization problem, producing Pareto front approximations whose characteristics are related to the QI on which they are based. In this paper, we propose a novel algorithm based on the island model that aims to take advantage of the cooperation of individual IB-MOEAs based on the indicators hypervolume, R2, IGD$^+$, ϵ^+, and Δ_p with the aim of improving both convergence and distribution of the Pareto fronts produced. Our experimental results, taking into account seven quality indicators, empirically show that the cooperation of several IB-MOEAs is better than using panmictic versions of them. Additionally, we also show that the performance of our proposal does not depend on the Pareto front shape of the problem being solved.

Index Terms—Multi-Objective Optimization, Quality Indicators, Island Model

I. INTRODUCTION

Many real-world problems can be mathematically defined as multi-objective optimization problems (MOPs), since they involve the simultaneous optimization of two or more conflicting objective functions. In general, an MOP is formally described as follows:

$$\min_{\vec{x}\in\Omega}\left\{\vec{F}(\vec{x}) = (f_1(\vec{x}),\ldots,f_m(\vec{x}))\right\}, \qquad (1)$$

where $\vec{x}$ is the vector of decision variables, $\Omega \subseteq \mathbb{R}^n$ is the feasible region set and $\vec{F}(\vec{x})$ is the vector of $m \geq 2$ objective functions where $f_i : \mathbb{R}^n \to \mathbb{R}$ for $i = 1,\ldots,m$. Due to the conflict among the objective functions, solving an MOP involves finding the best possible trade-offs among them. The particular set that yields the optimum values, according to the Pareto dominance relation[1] for all the objective functions is

known as the Pareto optimal set and its image is known as the Pareto optimal front ($\mathcal{PF}^*$).

In the last 30 years, Multi-Objective Evolutionary Algorithms (MOEAs) have become an increasingly popular approach to solve complex MOPs [1]. MOEAs originally adopted the Pareto dominance relation as their primary selection mechanism. However, it has been empirically shown that the selection pressure of Pareto-based MOEAs quickly dilutes when tackling MOPs having more than three objective functions, i.e., the so-called many-objective optimization problems (MaOPs). This has given rise to other types of MOEAs: those based on decomposition (which transform an MOP into several single-objective optimization problems which are solved simultaneously) [2] and those based on the use of quality indicators (QIs) [3].

QIs[2] are functions that quantitatively determine how good is a Pareto front approximation generated by an MOEA. According to Zitzler *et al.* [4], an approximation set[3] should ideally be as close as possible to $\mathcal{PF}^*$, covering it completely and having evenly distributed solutions. QIs aim to assess these desired features, i.e., convergence, spread and uniformity of solutions [5], [6]. In the specialized literature there is a plethora of QIs focused on assessing one or more desired aspects. A remarkable QI is the hypervolume indicator (HV) [7] that simultaneously assesses convergence and uniformity of solutions by measuring the volume dominated by an approximation set. On the other hand, the Riesz s-energy indicator [8], which is based on potential theory, measures the uniformity of solutions, being invariant to the shape of the manifold. Thus, as each QI is focused on specific aspects, they exhibit particular preferences over Pareto front approximations [9], [10]. For instance, on some specific MOPs, HV prefers approximation sets where solutions are closer to the Pareto front's knee [11].

The incorporation of QIs into the environmental selection, the density estimator or the archiver of an MOEA gave rise to the so-called indicator-based MOEAs (IB-MOEAs) [3], [12]–[14]. The underlying idea of these indicator-based selection

[1]Given $\vec{x}, \vec{y} \in \mathbb{R}^n$ and $\vec{F} : \mathbb{R}^n \to \mathbb{R}^m$, we say that $\vec{x}$ Pareto dominates $\vec{y}$ (denoted as $\vec{F}(\vec{x}) \prec \vec{F}(\vec{y})$) if and only if $\forall i = 1,\ldots,m, f_i(\vec{x}) \leq f_i(\vec{y})$ and there exists at least an index $j \in \{1,\ldots,m\}$ such that $f_j(\vec{x}) < f_j(\vec{y})$.

[2]Let $\mathcal{A} \subset \mathcal{PF}^*$ be an approximation set. A k-ary quality indicator is a function $I : (\mathcal{A}_1,\ldots,\mathcal{A}_k) \to \mathbb{R}$ which assigns a real value to a vector of k approximation sets.

[3]An approximation set is a set of mutually non-dominated vectors of objective function values.

mechanisms is to solve (or approximate) the indicator-based subset selection problem (IBSSP) [15], i.e., select from a set of $\mu + \lambda$ solutions, a subset of size μ that optimizes the QI. The vast majority of IB-MOEAs employ convergence-related QIs in their selection mechanisms, being HV the most important one, because among all classical indicators it is the only one that is Pareto-compliant[4]. However, its computational cost increases super-polynomially with the number of objectives. Thus, its use is prohibitive for MaOPs. In consequence, other less expensive convergence QIs such as R2 [16], Inverted Generational Distance plus (IGD$^+$) [17], additive ϵ indicator (ϵ^+) [6], and the Averaged Hausdorff Distance indicator (Δ_p) [18] have been successfully employed in MaOPs. As an IB-MOEA drives its population towards $\mathcal{PF}^*$ by tackling the IBSSP, the final population will exhibit characteristics strongly related to the preferences of its base QI. Due to this bias, the approximation sets of different IB-MOEAs for a specific MOP significantly vary.

Recently, an open research area that has attracted the attention of the evolutionary multi-objective optimization community is the design of MOEAs whose performance does not strongly depend on the Pareto front shapes. Ishibuchi *et al.* [19] pointed out that, currently, many MOEAs are overspecialized on benchmark problems whose Pareto fronts are strongly correlated with the shape of a simplex. In this paper, we propose an MOEA based on the island model [20] in which five steady-state IB-MOEAs based on the indicators HV, R2, IGD$^+$, ϵ^+, and Δ_p, and a Riesz s-energy-based archive cooperate. The goals of our proposed approach are twofold: (1) show that its performance does not depend on the Pareto front shapes, making it able to tackle MOPs with complicated Pareto fronts, and (2) empirically show that the cooperation of IB-MOEAs gives better results than the use of panmictic IB-MOEAs.

The remainder of this paper is organized as follows. Section II briefly introduces the QIs adopted in our proposed approach. In Section III, we describe the previous related work. Our proposal is outlined in Section IV and the experimental results are shown in Section V. Finally, our main conclusions and future work are sketched in Section VI.

II. QUALITY INDICATORS

In this section, we formally define the HV, R2, IGD$^+$, ϵ^+, Δ_p and Riesz s-energy (E_s) indicators. In all cases, let $\mathcal{A}$ be an approximation set and $\mathcal{Z}$ be a reference set. m is the dimension of the objective space.

Definition 1 (Hypervolume indicator): Given an anti-optimal reference point $\vec{r} \in \mathbb{R}^m$, the hypervolume is defined as follows:

$$HV(\mathcal{A}, \vec{r}) = \mathcal{L}\left(\bigcup_{\vec{a} \in \mathcal{A}} \left\{ \vec{b} \mid \vec{a} \prec \vec{b} \prec \vec{r} \right\} \right), \quad (2)$$

where $\mathcal{L}(\cdot)$ denotes the Lebesgue measure in $\mathbb{R}^m$.

[4]A (weakly) Pareto-compliant QI guarantees that the indicator values of one algorithm are better (or at least not worse) than another in case the approximation sets of the former (weakly) dominates the other's.

Definition 2 (Unary R2 indicator): The unary R2 indicator is defined as follows:

$$R2(\mathcal{A}, W) = -\frac{1}{|W|} \sum_{\vec{w} \in W} \max_{\vec{a} \in \mathcal{A}} \{u_{\vec{w}}(\vec{a})\}, \quad (3)$$

where W is a set of weight vectors and $u_{\vec{w}} : \mathbb{R}^m \to \mathbb{R}$ is a scalarizing function defined by $\vec{w} \in W$ that assigns a real value to each m-dimensional vector.

Definition 3 (IGD$^+$ indicator): The IGD$^+$, for minimization, is defined as follows:

$$IGD^+(\mathcal{A}, Z) = \frac{1}{|Z|} \sum_{\vec{z} \in Z} \min_{\vec{a} \in \mathcal{A}} d^+(\vec{a}, \vec{z}), \quad (4)$$

where $d^+(\vec{a}, \vec{z}) = \sqrt{\sum_{k=1}^{m} \left(\max\{a_k - z_k, 0\} \right)^2}$.

Definition 4 (Unary ϵ^+ indicator): The unary ϵ^+-indicator gives the minimum distance by which a Pareto front approximation needs to or can be translated in each dimension in objective space such that a reference set is weakly dominated. Mathematically, it is defined as follows:

$$\epsilon^+(\mathcal{A}, \mathcal{Z}) = \max_{\vec{z} \in \mathcal{Z}} \min_{\vec{a} \in \mathcal{A}} \max_{1 \leq i \leq m} \{z_i - a_i\}. \quad (5)$$

Definition 5 (Δ_p indicator): For a given $p > 0$, the Δ_p is defined as follows:

$$\Delta_p(\mathcal{A}, Z) = \max \{GD_p(\mathcal{A}, Z), IGD_p(\mathcal{A}, Z)\}. \quad (6)$$

Δ_p is defined on the basis of two indicators: GD$_p$ and IGD$_p$ which are slight modifications of the indicators Generational Distance (GD) [21] and Inverted Generational Distance (IGD) [22], respectively. These are defined in the following.

Definition 6 (GD$_p$ indicator):

$$GD_p(\mathcal{A}, \mathcal{Z}) = \left(\frac{1}{|\mathcal{A}|} \sum_{\vec{a} \in \mathcal{A}} d(\vec{a}, \mathcal{Z})^p \right)^{1/p}, \quad (7)$$

where $d(\vec{a}, \mathcal{Z}) = \min_{\vec{z} \in \mathcal{Z}} \sqrt{\sum_{i=1}^{m} (a_i - z_i)^2}$.

Definition 7 (IGD$_p$ indicator):

$$IGD_p(\mathcal{A}, \mathcal{Z}) = GD_p(\mathcal{Z}, \mathcal{A}) = \left(\frac{1}{|\mathcal{Z}|} \sum_{\vec{z} \in \mathcal{Z}} d(\vec{z}, \mathcal{A})^p \right)^{1/p}, \quad (8)$$

Definition 8 (Indicator contribution): Let $\mathcal{I}$ be any indicator in the set $\{HV, R2, IGD^+, \epsilon^+, \Delta_p\}$. The individual contribution C of a solution $\vec{a} \in \mathcal{A}$ to the indicator value is given as follows:

$$C_{\mathcal{I}}(\vec{a}, \mathcal{A}) = |\mathcal{I}(\mathcal{A}) - \mathcal{I}(\mathcal{A} \setminus \{\vec{a}\})|. \quad (9)$$

Definition 9 (Riesz s-energy): For a given $s > 0$, the Riesz s-energy indicator is defined as follows:

$$E_s(\mathcal{A}) = \sum_{i \neq j} \|\vec{a}_i - \vec{a}_j\|^{-s}, \quad (10)$$

as $s \to \infty$, E_s prefers more uniform solutions. This indicator measures the even distribution of a set of points in d-dimensional manifolds.

Definition 10 (Riesz s-energy individual contribution): The individual contribution C of a solution $\vec{a} \in \mathcal{A}$ to the Riesz s-energy indicator is as follows:

$$C_{E_s}(\vec{a}, \mathcal{A}) = \frac{1}{2} \left[E_s(\mathcal{A}) - E_s(\mathcal{A} \setminus \{\vec{a}\}) \right] \qquad (11)$$

III. PREVIOUS RELATED WORK

In this section, we briefly describe three IB-MOEAs that employ the indicators HV, R2 and IGD^+ as the core of their density estimators. A density estimator (DE) is the secondary selection criterion and its main goal is to break ties when solutions have the same dominance rank. Additionally, we outline a hyper-heuristic in which the best indicator-based DE (IB-DE), according to the problem being solved, is selected from a pool of IB-DEs.

The S-Metric Selection Evolutionary Multi-Objective Algorithm (SMS-EMOA) [3] is a steady-state MOEA that employs Pareto dominance as its main selection criterion, and it adopts a density estimator based on the HV indicator. At each generation, SMS-EMOA produces a single offspring which is added to the main population. This joint population is then divided into nondominated layers, using the nondominated sorting algorithm [23]. If the worst layer (the one that is dominated by all the remaining layers) has more than one solution, the HV-based density estimator is in charge of deleting the worst-contributing solution to the HV value. SMS-EMOA has been extensively tested on different benchmark problems, showing outstanding performance. Due to the HV preference, SMS-EMOA selects solutions close to the Pareto front's knee, although, for linear Pareto fronts, it produces evenly distributed solutions [11]. A recent study has empirically shown that the distributions produced by SMS-EMOA on each MOP strongly depend on the way in which the reference point is defined [24], i.e., the reference point is a preference information on preferable sets [25].

Following the SMS-EMOA scheme, the algorithms R2-EMOA [12] and IGD^+-Many Objective Evolutionary Algorithm (IGD^+-MaOEA) [13] have been proposed to reduce SMS-EMOA's computational cost and to exploit the properties of the R2 and IGD^+ indicators. The underlying idea of both R2-EMOA and IGD^+-MaOEA is to replace the HV-based density estimator by the corresponding QI of each IB-MOEA. On the one hand, R2-EMOA requires a set of convex weight vectors[5] as search directions and a scalarizing function (SF) because of the use of the R2 indicator. In concave and linear Pareto fronts, when using an adequated SF, R2-EMOA produces evenly distributed solutions. However, for disconnected, degenerated or for Pareto fronts which are not strongly correlated to the simplex form [19], R2-EMOA has several drawbacks because its convex weight vectors cannot intersect the Pareto front completely. On the other hand, Falcón-Cardona and Coello showed that the performance of IGD^+-MaOEA does not depend on the Pareto front shape. IGD^+-MaOEA was one of the first algorithms tested on the

---

[5]A weight vector $\vec{w}$ is a convex weight vector if and only if $\sum_{i=1}^{m} w_i = 1$ and $w_i \geq 0, i = 1, \ldots, m$.
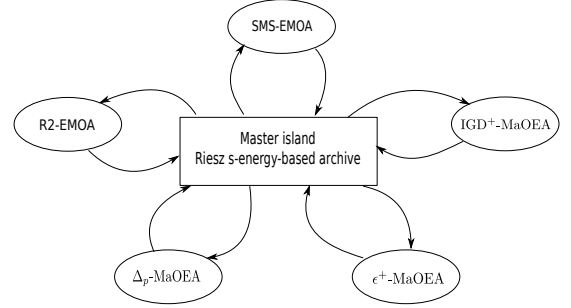

Fig. 1. cMIB-MOEA is composed of five islands (each one executing a specific IB-MOEA) and a master island that manages a Riesz s-energy-based archive. The communication between the master island and the other islands is bidirectional.

Deb-Thiele-Laumanns-Zitzler minus ($DTLZ^{-1}$) benchmarks which was proposed by Ishibuchi *et al.* [19]. However, IGD^+-MaOEA is not able to produce evenly distributed solutions in most problems. In some cases, for example, when dealing with concave Pareto fronts, the distributions of IGD^+-MaOEA are similar to those of SMS-EMOA.

In 2018, Falcón-Cardona and Coello proposed the Multi-Indicator Hyper-heuristic (MIHPS) whose main idea is to select the best IB-DE from the pool {R2-DE, IGD^+-DE, ϵ^+-DE, Δ_p-DE}, depending on the MOP being solved. MIHPS is based on the SMS-EMOA framework, but it probabilistically selects a new IB-DE every T_w iterations. This decision is biased by the past performance of the IB-DE on the global convergence of MIHPS. If the IB-DE helped to improve convergence, its selection probability is rewarded. Otherwise, it is penalized. The experimental results showed that MIHPS tends to prefer IGD^+-DE, ϵ^+-DE and Δ_p-DE during the first evolutionary stages and prefers R2-DE in the last generations. Based on these results, the behavior of MIHPS is controlled by an internal competition between all the IB-DEs. In other words, each IB-DE competes with the others to be selected as much as possible, which means that it has to produce better convergence behavior in comparison with the remaining heuristics. Hence, at the end of the evolutionary process, the advantages and also the drawbacks of a single IB-DE are predominant.

IV. OUR PROPOSED APPROACH

In this section, we describe our proposal, called Cooperative Multi-Indicator-based MOEA (cMIB-MOEA). Our proposed cMIB-MOEA relies on the cooperation of five IB-MOEAs: SMS-EMOA, R2-EMOA, IGD^+-MaOEA and two more IB-MOEAs very similar to IGD^+-MaOEA but using the indicators ϵ^+ and Δ_p that are denoted as ϵ^+-MaOEA and Δ_p-MaOEA, respectively. To make possible the cooperation between the IB-MOEAs, cMIB-MOEA uses an island model as shown in Fig. 1. Additionally, a Riesz s-energy-based archive $\mathcal{A}$ is employed to maintain uniformly distributed solutions coming from the IB-MOEAs. Algorithm 1 outlines the master island that controls each island associated with an IB-DE, and it also manages $\mathcal{A}$. cMIB-MOEA requires as a parameter a

set of indicators; in our case, we use HV, R2, IGD$^+$, ϵ^+, and Δ_p. Each indicator is associated with the above mentioned IB-MOEAs. For each indicator $I_j, j = 1, \ldots, k$, a subpopulation P_j of size μ/k is randomly initialized, where μ is the size of $\mathcal{A}$. Additionally, the structures of the jth IB-MOEA are also initialized. Then, in line 5, the set of nondominated solutions extracted from all the subpopulations is used to initialize $\mathcal{A}$. Lines 6 to 15 outline the main loop of cMIB-MOEA. First, all the IB-MOEAs are independently executed during $fmig$ generations, using Algorithm 2, to updating their corresponding subpopulations. In line 9, the current archive is combined with all the subpopulations and, then, the set of nondominated solutions is extracted. If the contents of the archive is greater than μ, a density estimator based on the Riesz s-energy indicator is applied to reduce its size to μ. Finally, in line 15, the migration process, described in Algorithm 3, is executed. cMIB-MOEA returns the archive as its final solution set. In the following, we describe Algorithms 2 and 3.

Algorithm 1 cMIB-MOEA general framework

Require: Number $nmig$ of solutions to migrate; migration frequency $fmig$; Population size μ; Set of indicators $\mathcal{I} = \{I_1, \ldots, I_k\}$
Ensure: Pareto front approximation
1: Set archive $\mathcal{A}$ as empty
2: **for** $j = 1$ to k **do**
3:    Randomly initialize subpopulation P_j of size μ/k
4:    Initialize the jth IB-MOEA
5: $\mathcal{A} \leftarrow Nondominated(\bigcup_{j=1}^{k} P_j)$
6: **while** stopping criterion is not fulfilled **do**
7:    **for** $j = 1$ to k **do**
8:       $P_j \leftarrow$ IB-MOEA$(P_j, I_j, fmig)$
9:    $\mathcal{A} \leftarrow \mathcal{A} \cup \left\{\bigcup_{j=1}^{k} P_j\right\}$
10:   $\mathcal{A} \leftarrow Nondominated(\mathcal{A})$
11:   Obtain $\vec{z}^*$ and $\vec{z}^{\text{nad}}$ from $\mathcal{A}$ to normalize $\mathcal{A}$
12:   **while** $|\mathcal{A}| > \mu$ **do**
13:      $\vec{a}_{\text{worst}} \leftarrow \arg\max_{\vec{a} \in \mathcal{A}} C_{E_s}(\vec{a}, \mathcal{A})$
14:      $\mathcal{A} \leftarrow \mathcal{A} \setminus \{\vec{a}_{\text{worst}}\}$
15:   $\{P_1, \ldots, P_k\} \leftarrow$ Migration$(nmig, \{P_1, \ldots, P_k\}, \{I_1, \ldots, I_k\})$
16: **return** $\mathcal{A}$

Algorithm 2 describes the general framework proposed by Beume *et al.* in SMS-EMOA [3]. However, in this case, we describe it in a generic way so that the IB-MOEA works with a given indicator I from the set $\{$HV, R2, IGD$^+$, ϵ^+, $\Delta_p\}$. Since each IB-MOEA is executed at every step of cMIB-MOEA during $fmig$ generations, this number is the stopping condition of the loop in line 2. At every generation, a single offspring is generated and, then, added to the main population. The joint population Q is ranked, using the nondominated sorting algorithm to produce the layers $R1, \ldots, R_t$, where R_t has the worst solutions according to the Pareto dominance relation. If this layer has more than one solution, all the individual contributions to the indicator I are calculated using equation (9) and obtaining the solution $\vec{r}_{\text{worst}}$ with the minimal C value. Then, $\vec{r}_{\text{worst}}$ is deleted from Q and P is updated in line 11.

The migration process of cMIB-MOEA is rather simple. If the archive has more than $nmig$ solutions, then migration is possible. To the jth population, we only migrate solutions

---

Algorithm 2 Generic steady-state IB-MOEA

Require: Population P; Indicator I; migration frequency $fmig$
Ensure: Updated population P
1: $g \leftarrow 0$
2: **while** $g < fmig$ **do**
3:    Generate offspring $\vec{q}$ from population P
4:    $Q \leftarrow P \cup \{\vec{q}\}$
5:    Obtain $\vec{z}^*$ and $\vec{z}^{\text{nad}}$ from Q and normalize it
6:    $\{R_1, \ldots, R_t\} \leftarrow NDsorting(Q)$
7:    **if** $|R_t| > 1$ **then**
8:       $\vec{r}_{\text{worst}} \leftarrow \arg\min_{\vec{r} \in R_t} C_I(\vec{r}, R_t)$
9:    **else**
10:      $\vec{r}_{\text{worst}}$ is the single solution in R_t
11:   $P \leftarrow Q \setminus \{\vec{r}_{\text{worst}}\}$
12:   $g \leftarrow g + 1$
13: **return** P

---

from $\mathcal{A}$ that were not produced by the jth IB-MOEA. In other words, P_j can receive solutions from all other populations $P_i, i \neq j$. The selection of the $nmig$ solutions to be migrated to P_j is randomized. The selected $nmig$ solutions will replace the worst $nmig$ contributing solutions to the indicator I_j, previously computed. In this case, we employ an elitist replacement scheme.

Algorithm 3 Migration

Require: Number $nmig$ of solutions to migrate; Set of subpopulations $\{P_1, \ldots, P_k\}$; Set of indicators $\{I_1, \ldots, I_k\}$
Ensure: Updated subpopulations
1: **if** $|\mathcal{A}| > nmig$ **then**
2:    **for** $j = 1$ to k **do**
3:       **if** there are $nmig$ solutions in $\mathcal{A}$ that were not produced by the jth IB-MOEA **then**
4:          Randomly select $nmig$ solutions from $\mathcal{A}$ that were not generated by the jth IB-MOEA
5:          Replace from P_j its $nmig$ worst-contributing solutions to I_j, using the previously selected solutions
6: **return** $\{P_1, \ldots, P_k\}$

An essential aspect that it is worth to emphasize is why we employ SMS-EMOA in spite of its high computational cost. Hernández and Coello [26] empirically showed that when using SMS-EMOA with micro-populations, i.e., populations of no more than 30 individuals, then, the running time of SMS-EMOA remains relatively constant although the number of objective functions increases. Based on this fact, we set the size of each subpopulation equals to μ/k such that this number does not exceed 30 individuals.

V. EXPERIMENTAL RESULTS

In this section, we analyze the performance of cMIB-MOEA[6] when compared to panmictic versions of SMS-EMOA, R2-EMOA, IGD$^+$-MaOEA, ϵ^+-MaOEA, and Δ_p-MaOEA. We adopted MOPs from the Deb-Thiele-Laumanns-Zitzler (DTLZ) [27], Walking-Fish-Group (WFG) [28], Lamé superspheres [29], Viennet (VIE) [21], and the DTLZ^{-1} and WFG^{-1} test suites [19]. Table I summarizes the MOPs that we

---

employed for two and three objective functions, emphasizing their Pareto front shapes. For each test instance, we performed 30 independent executions. The performance of cMIB-MOEA and the adopted IB-MOEAs was compared using the quality indicators HV, R2, IGD$^+$, ϵ^+, Δ_p. However, as each of these QIs prefers the IB-MOEA that uses it as its IB-DE, we decided to leave aside that IB-MOEA for a fair comparison. For example, when comparing performance using HV, we included all the adopted IB-MOEAs except for SMS-EMOA. Additionally, we employed the Hausdorff distance as a neutral convergence measure and the Solow-Polasky indicator for diversity [30].

A. Parameters settings

For a fair comparison, cMIB-MOEA and the other IB-MOEAs use the same population size μ as described in Table II. For both two and three objective functions $\mu = C_{m-1}^{H^1+m-1}$, where this combinatorial number determines how many convex weight vectors (as required by R2-EMOA) are generated via the Simplex-Lattice-Design method. All subpopulations are set to $\mu/5$, where five is the number of subpopulations. The stopping criterion of all the MOEA is the maximum number of function evaluations (MaxFeval). Additionally, Table II indicates the $fmig$ and $nmig$ parameters of cMIB-MOEA. All the adopted IB-MOEAs utilize Simulated Binary Crossover (SBX) and polynomial-based mutation as their variation operators. In all cases, the crossover probability and the mutation probability were set to 0.9 and $1/n$ (where n is the number of decision variables), respectively. Both the crossover distribution index and the mutation distribution index are equal to 20. Regarding the MOPs, the number of variables of problems DTLZ, DTLZ^{-1}, Lamé and Mirror is $n = m + K - 1$, where $K = 10$ for DTLZ2 and DTLZ5 and their minus versions, $K = 20$ for DTLZ7 and DTLZ7^{-1}, and $K = 5$ in all Lamé and Mirror instances that are determined by a different γ value as shown in Table I. Considering the WFG and WFG^{-1} problems, the number of variables are 24 and 26 for two and three objectives, respectively, in both cases the number of position-related parameters is two. The decision space of the three Viennet problem is of dimension two.

B. Discussion of results

The comparison of cMIB-MOEA with the panmictic IB-MOEAs has two main goals: 1) determine that the cooperation between IB-MOEAs produces better global results, and 2) show that cMIB-MOEA is a more general multi-objective optimizer. Regarding the first goal, we compared the performance of cMIB-MOEA with the other IB-MOEAs using the QIs: HV, R2, IGD$^+$, ϵ^+, Δ_p, Hausdorff distance and the Solow Polasky indicator. From these QIs, the Hausdorff distance is the only neutral convergence measure, i.e., none of the MOEAs uses it as an IB-DE. Table III shows the mean and standard deviation of all IB-MOEAs on each test instance, regarding the Hausdorff distance. It is worth noting that the reference set required by this metric (and also by IGD$^+$, ϵ^+, and Δ_p) was built uniformly sampling the true Pareto front of

TABLE I
ADOPTED MOPS IN THE STUDY. FOR EACH CASE, THE PARETO FRONT GEOMETRY IS DESCRIBED, INDICATING IF IT IS CORRELATED WITH THE SHAPE OF A SIMPLEX.

MOP	Pareto front shape	Simplex-like
DTLZ2	Concave	Yes
DTLZ2^{-1}	Convex	No
DTLZ5	Degenerate	No
DTLZ5^{-1}	Convex	No
DTLZ7	Disconnected	No
DTLZ7^{-1}	Disconnected	No
WFG1	Mixed	Yes
WFG1^{-1}	Mixed	No
WFG2	Disconnected	Yes
WFG2^{-1}	Slightly concave	No
WFG3	Degenerate	No
WFG3^{-1}	Linear	No
Lamé $\gamma = 0.25$	Highly convex	No
Lamé $\gamma = 1.00$	Linear	Yes
Lamé $\gamma = 5.00$	Highly concave	Yes
Mirror $\gamma = 0.25$	Highly concave	No
Mirror $\gamma = 1.00$	Linear	No
Mirror $\gamma = 5.00$	Highly convex	No
VIE1	Convex	No
VIE2	Mixed (convex and degenerate)	No
VIE3	Degenerate	No

TABLE II
PARAMETERS ADOPTED IN THE COMPARISON. H^1 AND H^2 ARE THE PARAMETERS FOR THE GENERATION OF THE SET OF WEIGHT VECTORS OF THE R2-EMOA USED BY CMIB-MOEA AND THE CORRESPONDING PANMICTIC VERSION.

Dim.	H^1	H^2	μ	$\mu/5$	Maxfeval	$fmig$	$nmig$
2	19	99	100	20	50,000	20	5
3	5	13	105	21	60,000	21	5

all problems, producing sets of size 200 and 300 for two- and three-dimensional MOPs, respectively. From Table III, cMIB-MOEA is the best optimizer since it obtained the best value in 14 out of 39 problems while SMS-EMOA obtained the second-ranked MOEA, having the best result in 9 out of 39 MOPs. In order to reinforce the evidence that the cooperation between the individual IB-MOEAs benefits cMIB-MOEA, we also compared it using their baseline QIs, i.e., HV, R2, IGD$^+$, ϵ^+, and Δ_p. Due to space limitations, we do not show the numerical tables[7] here, but we summarize the results in Fig. 3. This figure is a heat map that shows the number of times that each IB-MOEA was ranked first or second according to the above mentioned QIs. Based on this figure, cMIB-MOEA is also the best optimizer regarding the HV, R2, and Δ_p indicators, and it obtained the second place for IGD$^+$ and ϵ^+. cMIB-MOEA obtained the first place in 27 out of 39 MOPs, regarding HV while for both R2 and Δ_p, it is the best MOEA in 22 test instances. As we explained above, the decision of leaving aside, for example, SMS-EMOA when making an HV-based comparison is to avoid the preference that HV has

---

[7]The complete study is available at http://computacion.cs.cinvestav.mx/cMIB-MOEA/cMIB-MOEA.html.
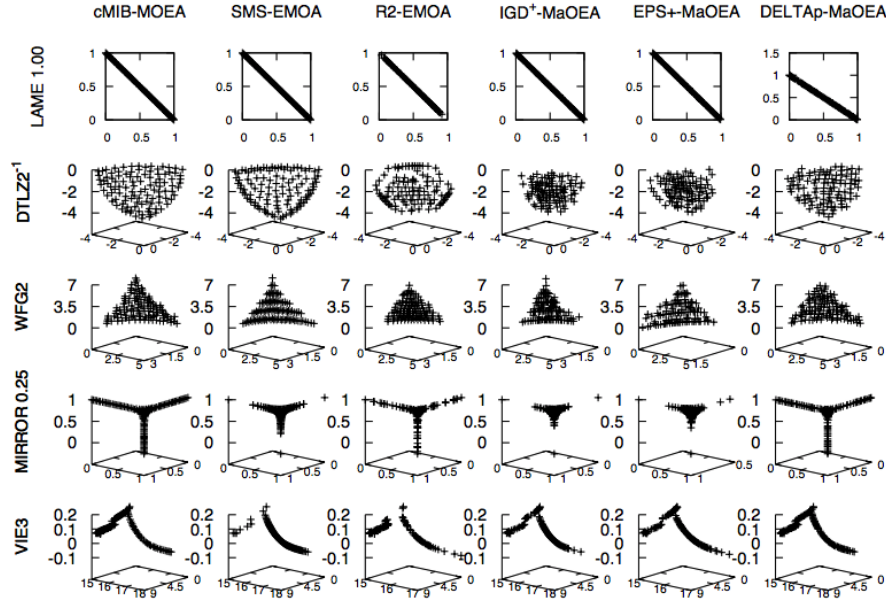
Fig. 2. Pareto fronts generated by cMIB-MOEA and the adopted IB-MOEAs. Each front corresponds to the median of the Solow Polasky value.

towards SMS-EMOA and, with the aim of providing unbiased results. In the light of the experimental results, we have the first insight that the cooperation between individual IB-MOEAs instead of using panmictic versions of them, improves the quality of an optimizer. Since each individual IB-MOEA is exploring and exploiting different regions of the Pareto front, according to its QI-based preferences, cMIB-MOEA takes advantage of the strengths of each IB-MOEA to improve the global behavior. Additionally, we performed some experiments in order to determine the impact of the migration process, and we concluded that it helps to improve the search progress. In consequence, we claim that the cooperation is the responsible for getting better results, since cMIB-MOEA is the best optimizer in four out of six convergence measures, i.e., HV, R2, Δ_p, and the Hausdorff Distance and it gets the second place in the remaining ones, i.e., IGD^+ and ϵ^+.

The second goal of our experiments is to obtain evidence showing that cMIB-MOEA is a more general optimizer, i.e., that its performance does not depend on the Pareto front shape as it happens with other MOEAs [19]. Once we know that cMIB-MOEA had better convergence results, it is possible to analyze the Pareto fronts of all the adopted IB-MOEAs using the Solow Polasky Diversity indicator (SPD). Fig. 3 reveals that distributions generated by cMIB-MOEA have the best SPD value in 33 out of 39 test instances. In consequence, cMIB-MOEAs outperforms the panmictic versions of SMS-EMOA, R2-EMOA, IGD^+-MaOEA, ϵ^+-MaOEA, and Δ_p-MaOEA, which indicates that its performance is good when dealing with complex Pareto front shapes as shown in Table I. Figure 2 shows a comparison of Pareto fronts produced by cMIB-MOEA and the adopted IB-MOEAs. From this figure, we can see that the cMIB-MOEA produces evenly distributed Pareto fronts independently of the associated geometry. This
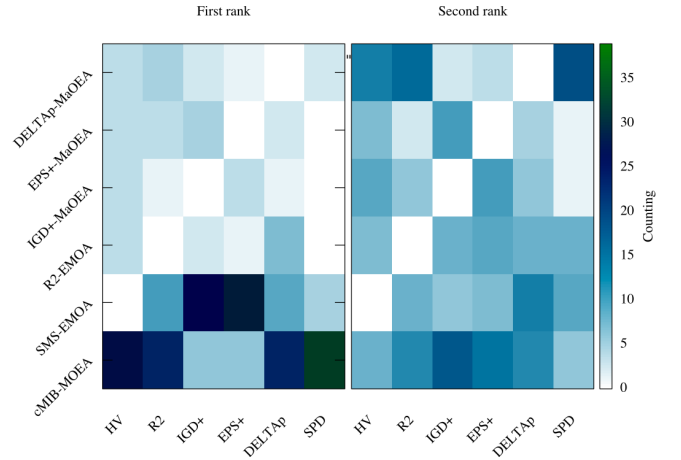

Fig. 3. Heat map that revels the number of times an IB-MOEA was ranked first or second according to the indicators HV, R2, IGD^+, ϵ^+, Δ_p, and Solow Polasky (SPD).

behavior is not as evident in the other IB-MOEAs.

VI. CONCLUSIONS

In this paper, we proposed an MOEA based on the island model that takes advantage of the cooperation of five indicator-based MOEAs and one archive based on the Riesz s-energy indicator. The adopted IB-MOEAs are SMS-EMOA, R2-EMOA, IGD^+-MaOEA, ϵ^+-MaOEA, and Δ_p-MaOEA, based on the indicators HV, R2, IGD^+, ϵ^+, and Δ_p, respectively. Based on our experimental results, we empirically showed that our approach, denoted as cMIB-MOEA, is better than panmictic versions of the individual IB-MOEAs and it also is a more general optimizer since its performance does not depend on the Pareto front shapes. As part of our future work, we are

Problema	Dim.	cMIB-MOEA	SMS-EMOA	R2-EMOA	IGD$^+$-MaOEA	ϵ^+-MaOEA	Δ_p-MaOEA
DTLZ2	2	1.105384e-02 (9.270729e-04)	3.173838e-02# (1.613701e-03)	9.590904e-03 (1.391367e-04)	5.901683e-02# (8.997635e-03)	5.888548e-02# (1.039106e-02)	2.202810e-02# (1.382455e-02)
	3	1.092411e-01 (5.923393e-03)	1.594444e-01# (4.319644e-03)	9.818462e-02 (4.189210e-04)	1.976556e-01# (1.981525e-02)	1.924996e-01# (2.326289e-02)	1.390080e-01# (1.353515e-02)
DTLZ2^{-1}	2	3.788524e-02 (2.808735e-03)	7.352529e-02# (4.638478e-03)	1.631498e+00# (2.864086e-01)	3.803191e-01# (9.505168e-02)	3.970059e-01# (9.754773e-02)	6.172824e-02# (7.946931e-03)
	3	3.699226e-01 (1.824022e-02)	4.168909e-01# (1.539622e-02)	1.384586e+00# (1.464603e-01)	1.289982e+00# (1.636542e-01)	1.288563e+00# (1.892405e-01)	5.732136e-01# (9.746681e-02)
DTLZ5	2	1.144525e-02 (2.091661e-03)	3.121338e-02# (1.973508e-03)	9.483349e-03 (1.314487e-04)	5.586760e-02# (9.183465e-03)	6.197110e-02# (1.253256e-02)	1.841037e-02# (5.364925e-03)
	3	1.222078e-02 (4.516118e-03)	3.331912e-02# (1.979639e-03)	7.259896e-02# (3.636487e-02)	5.756635e-02# (1.250585e-02)	5.937786e-02# (1.155631e-02)	1.846343e-02# (3.622081e-03)
DTLZ5^{-1}	2	3.811842e-02 (2.470698e-03)	7.833632e-02# (4.100489e-03)	1.611194e+00# (2.759175e-01)	3.779225e-01# (1.242316e-01)	4.104359e-01# (1.043483e-01)	6.285257e-02# (1.445305e-02)
	3	3.144057e-01 (1.871137e-02)	3.854935e-01# (1.594254e-02)	1.375219e+00# (2.965503e-01)	1.158550e+00# (1.802020e-01)	1.223359e+00# (2.628891e-01)	5.038938e-01# (1.127651e-01)
DTLZ7	2	6.069350e-02 (2.496451e-01)	2.115424e-02 (1.394340e-03)	5.462852e-02 (6.044351e-02)	7.816969e-02# (2.465541e-01)	3.257727e-02 (7.789854e-03)	3.384385e-02 (2.748613e-02)
	3	3.477614e-01 (4.239738e-01)	6.813853e-01# (4.366072e-01)	3.168888e-01 (2.950831e-01)	4.690831e-01# (3.918240e-01)	6.705290e-01# (6.218506e-01)	6.520370e-01# (5.645169e-01)
DTLZ7^{-1}	2	8.858600e-03 (4.680836e-03)	1.180794e-02# (1.042123e-03)	3.498117e-02# (1.530521e-02)	1.713431e-02# (5.742480e-03)	1.656072e-02# (4.531754e-03)	1.278824e-02# (2.264126e-03)
	3	5.376569e-01 (1.845419e-01)	5.226155e-01 (1.108634e-01)	5.009742e-01 (1.179733e-01)	5.716971e-01# (1.722787e-01)	5.834904e-01# (1.787834e-01)	5.136677e-01 (1.140769e-01)
WFG1	2	1.872677e+00 (6.490135e-01)	2.144039e+00# (4.656587e-01)	2.781527e+00# (4.513154e-01)	2.084150e+00# (5.979649e-01)	2.274507e+00# (2.864709e-01)	2.260408e+00# (2.907941e-01)
	3	2.779055e+00 (3.589481e-01)	2.299031e+00 (2.955950e-01)	2.842268e+00# (3.041895e-01)	3.108680e+00# (3.236080e-01)	3.227137e+00# (1.808980e-01)	3.084785e+00# (3.347422e-01)
WFG1^{-1}	2	2.193076e+00 (6.692088e-01)	2.460818e+00# (3.054873e-01)	3.587648e+00# (3.319739e-02)	2.425964e+00# (5.121160e-01)	2.487955e+00# (5.919251e-01)	2.010333e+00# (7.165466e-01)
	3	3.023132e+00 (7.234743e-01)	3.178590e+00# (4.988111e-01)	3.663829e+00# (3.787046e-02)	3.568923e+00# (1.927237e-01)	3.704674e+00# (4.030209e-02)	3.484878e+00# (2.869542e-01)
WFG2	2	6.510102e-01 (4.642023e-01)	7.509476e-01# (4.184325e-01)	7.049981e-01# (3.837817e-01)	8.250346e-01# (3.655739e-01)	5.792721e-01 (4.581925e-01)	7.594202e-01# (4.075064e-01)
	3	1.478811e+00 (1.087477e-01)	1.992816e+00# (6.342904e-02)	1.977591e+00# (5.231918e-02)	2.117238e+00# (1.639465e-01)	2.142116e+00# (2.007878e-01)	1.461806e+00 (2.294549e-01)
WFG2^{-1}	2	2.872757e-02 (3.355407e-03)	2.506092e-02 (1.060659e-03)	1.617072e-01# (6.794276e-02)	4.626452e-02# (7.036978e-03)	4.659729e-02# (7.037695e-03)	4.722215e-02# (5.741114e-03)
	3	4.547563e-01 (3.543713e-02)	1.343296e+00# (6.894212e-02)	7.481390e-01# (6.541303e-02)	9.564823e-01# (1.533654e-01)	9.681967e-01# (1.663861e-01)	6.546428e-01# (1.130453e-01)
WFG3	2	3.433451e-02 (2.669749e-03)	2.694516e-02 (1.619053e-03)	5.124899e-01# (1.930205e-01)	5.335781e-02# (1.258117e-02)	4.742735e-02# (1.091492e-02)	5.758475e-02# (1.446585e-02)
	3	2.153750e+00 (3.335947e-02)	2.094386e+00 (4.249273e-02)	2.120770e+00 (4.575346e-02)	1.437151e+00 (1.419643e-01)	1.394558e+00 (1.555797e-01)	1.737576e+00 (1.254863e-01)
WFG3^{-1}	2	3.115905e-02 (2.233907e-03)	2.413419e-02 (8.927896e-04)	4.257092e-01# (1.720072e-01)	5.551999e-02# (1.297264e-02)	5.153979e-02# (1.523855e-02)	5.393184e-02# (1.070818e-02)
	3	3.271397e-01 (1.790222e-02)	4.234791e-01# (2.478000e-02)	5.930895e-01# (9.457878e-02)	4.351743e-01# (4.216730e-01)	5.659076e-01# (1.642249e-01)	4.833494e-01# (1.070514e-01)
LAME $\gamma = 0.25$	2	1.022964e-01 (4.251508e-04)	7.199513e-02 (1.597357e-03)	7.790940e-01# (5.055874e-02)	4.493894e-01# (6.963783e-02)	4.163650e-01# (8.842754e-02)	1.076818e-01# (1.009479e-02)
	3	2.181521e-01 (9.166538e-02)	3.306315e-01# (4.715269e-02)	7.909163e-01# (3.595584e-02)	7.110521e-01# (4.389321e-02)	7.342863e-01# (2.043919e-02)	2.176095e-01 (5.148371e-02)
LAME $\gamma = 1.00$	2	1.233049e-02 (1.295561e-02)	7.492362e-03 (2.686326e-04)	9.955142e-02# (5.413129e-02)	1.391223e-02 (2.157235e-03)	1.414534e-02# (2.384110e-03)	1.657829e-02# (4.202435e-03)
	3	8.615970e-02 (1.671945e-02)	7.227939e-02 (4.298681e-03)	6.209480e-02 (4.602889e-03)	1.097183e-01# (1.840681e-02)	1.210148e-01# (2.856508e-02)	1.039719e-01# (1.373382e-02)
LAME $\gamma = 5.00$	2	3.559403e-02 (1.292145e-03)	1.401908e-01# (1.961413e-03)	3.420893e-02 (7.261769e-05)	2.214712e-01# (1.573873e-02)	2.128242e-01# (1.431933e-02)	3.450596e-02 (2.787760e-03)
	3	1.350820e-01 (8.562792e-03)	3.581202e-01# (9.384830e-03)	1.500124e-01# (2.721855e-04)	4.019987e-01# (1.775541e-02)	3.900596e-01# (3.091858e-02)	1.837234e-01# (2.418483e-02)
MIRROR $\gamma = 0.25$	2	4.790673e-02 (2.298588e-03)	1.691297e-01# (4.416528e-03)	4.996473e-02 (3.078737e-05)	2.797045e-01# (1.626290e-02)	2.887144e-01# (2.052701e-02)	4.789617e-02 (2.289451e-03)
	3	4.546330e-02 (4.264168e-03)	2.399739e-01# (3.823196e-03)	9.488459e-02# (1.195802e-02)	3.408904e-01# (1.539832e-02)	4.277988e-01# (1.271120e-01)	4.936646e-02# (5.774740e-03)
MIRROR $\gamma = 1.00$	2	9.824648e-03 (8.012889e-04)	7.610307e-03 (2.856453e-04)	8.211471e-02# (4.629837e-02)	1.297673e-02# (1.605581e-03)	1.339788e-02# (2.260016e-03)	1.584752e-02# (3.354279e-03)
	3	8.149582e-02 (4.428020e-03)	9.869028e-02# (3.037584e-03)	1.355981e-01# (1.433308e-02)	1.017920e-01# (1.173971e-02)	1.077039e-01# (1.064985e-02)	1.177466e-01# (2.897291e-02)
MIRROR $\gamma = 5.00$	2	6.923700e-02 (3.416160e-03)	5.861688e-02 (1.416267e-03)	7.132397e-01# (5.417028e-02)	3.364190e-01# (4.422825e-02)	3.267493e-01# (5.924901e-02)	6.846537e-02 (4.729740e-03)
	3	1.304210e-01 (8.209513e-03)	3.406023e-01# (3.904404e-03)	7.781739e-01# (2.151215e-02)	7.651215e-01# (5.207308e-02)	7.749160e-01# (4.590298e-02)	2.092879e-01# (2.264808e-02)
VIE1	3	1.552675e+00 (7.068297e-02)	1.474508e+00 (5.003594e-03)	1.165155e+00 (2.271376e-01)	1.086031e+00 (3.372768e-01)	1.112837e+00 (3.207447e-01)	1.556628e+00 (9.208280e-02)
VIE2	3	6.330866e-02 (1.959696e-02)	8.020737e-02# (7.431943e-03)	4.439421e-01# (2.447103e-01)	5.004996e-01# (1.673603e-01)	5.041798e-01# (1.984323e-01)	6.229146e-02 (1.629636e-02)
VIE3	3	3.597395e+01 (6.800830e-03)	3.597358e+01 (2.920827e-03)	3.578840e+01 (1.476454e-01)	3.575047e+01 (1.663358e-01)	3.575928e+01 (1.427880e-01)	3.595831e+01 (2.397284e-02)

interested in a more in-depth study of the behavior of cMIB-MOEA, focusing on the impact of the migration mechanisms in order to speed up convergence. We are also interested in studying the behavior of cMIB-MOEA when tackling many-objective optimization problems.

References

[1] C. A. Coello Coello, G. B. Lamont, and D. A. Van Veldhuizen, *Evolutionary Algorithms for Solving Multi-Objective Problems*, 2nd ed. New York: Springer, September 2007, iSBN 978-0-387-33254-3.

[2] Q. Zhang and H. Li, "MOEA/D: A Multiobjective Evolutionary Algorithm Based on Decomposition," *IEEE Transactions on Evolutionary Computation*, vol. 11, no. 6, pp. 712–731, December 2007.

[3] N. Beume, B. Naujoks, and M. Emmerich, "SMS-EMOA: Multiobjective selection based on dominated hypervolume," *European Journal of Operational Research*, vol. 181, no. 3, pp. 1653–1669, 16 September 2007.

[4] E. Zitzler, K. Deb, and L. Thiele, "Comparison of Multiobjective Evolutionary Algorithms: Empirical Results," Computer Engineering and Networks Laboratory (TIK), Swiss Federal Institute of Technology (ETH) Zurich, Gloriastrasse 35, CH-8092 Zurich, Switzerland, Tech. Rep. 70, December 1999.

[5] J. Knowles and D. Corne, "On Metrics for Comparing Nondominated Sets," in *Congress on Evolutionary Computation (CEC'2002)*, vol. 1. Piscataway, New Jersey: IEEE Service Center, May 2002, pp. 711–716.

[6] E. Zitzler, L. Thiele, M. Laumanns, C. M. Fonseca, and V. G. da Fonseca, "Performance Assessment of Multiobjective Optimizers: An Analysis and Review," *IEEE Transactions on Evolutionary Computation*, vol. 7, no. 2, pp. 117–132, April 2003.

[7] E. Zitzler and L. Thiele, "Multiobjective Optimization Using Evolutionary Algorithms—A Comparative Study," in *Parallel Problem Solving from Nature V*, A. E. Eiben, Ed. Amsterdam: Springer-Verlag, September 1998, pp. 292–301.

[8] D. P. Hardin and E. B. Saff, "Discretizing Manifolds via Minimum Energy Points," *Notices of the AMS*, vol. 51, no. 10, pp. 1186–1194, 2004.

[9] S. Jiang, Y.-S. Ong, J. Zhang, and L. Feng, "Consistencies and Contradictions of Performance Metrics in Multiobjective Optimization," *IEEE Transactions on Cybernetics*, vol. 44, no. 12, pp. 2391–2404, December 2014.

[10] A. Liefooghe and B. Derbel, "A Correlation Analysis of Set Quality Indicator Values in Multiobjective Optimization," in *2016 Genetic and Evolutionary Computation Conference (GECCO'2016)*. Denver, Colorado, USA: ACM Press, 20-24 July 2016, pp. 581–588, iSBN 978-1-4503-4206-3.

[11] A. Auger, J. Bader, D. Brockhoff, and E. Zitzler, "Theory of the Hypervolume Indicator: Optimal $\{\mu\}$-Distributions and the Choice of the Reference Point," in *FOGA '09: Proceedings of the tenth ACM SIGEVO workshop on Foundations of genetic algorithms*. Orlando, Florida, USA: ACM, January 2009, pp. 87–102.

[12] D. Brockhoff, "A Bug in the Multiobjective Optimizer IBEA: Salutary Lessons for Code Release and a Performance Re-Assessment," in *Evolutionary Multi-Criterion Optimization, 8th International Conference, EMO 2015*, A. Gaspar-Cunha, C. H. Antunes, and C. Coello Coello, Eds. Guimarães, Portugal: Springer. Lecture Notes in Computer Science Vol. 9018, March 29 - April 1 2015, pp. 187–201.

[13] J. G. Falcón-Cardona and C. A. Coello Coello, "Towards a More General Many-objective Evolutionary Optimizer," in *Parallel Problem Solving from Nature – PPSN XV, 15th International Conference, Proceedings, Part I*. Coimbra, Portugal: Springer. Lecture Notes in Computer Science Vol. 11101, September 8–12 2018, pp. 335–346, iSBN: 978-3-319-99258-7.

[14] ——, "A Multi-Objective Evolutionary Hyper-Heuristic Based on Multiple Indicator-Based Density Estimators," in *2018 Genetic and Evolutionary Computation Conference (GECCO'2018)*. Kyoto, Japan: ACM Press, July 15–19 2018, pp. 633–640, iSBN: 978-1-4503-5618-3.

[15] M. Basseur, B. Derbel, A. Goeffon, and A. Liefooghe, "Experiments on Greedy and Local Search Heuristics for d-Dimensional Hypervolume Subset Selection," in *2016 Genetic and Evolutionary Computation Conference (GECCO'2016)*. Denver, Colorado, USA: ACM Press, 20-24 July 2016, pp. 541–548, iSBN 978-1-4503-4206-3.

[16] D. Brockhoff, T. Wagner, and H. Trautmann, "On the Properties of the $R2$ Indicator," in *2012 Genetic and Evolutionary Computation Conference (GECCO'2012)*. Philadelphia, USA: ACM Press, July 2012, pp. 465–472, iSBN: 978-1-4503-1177-9.

[17] H. Ishibuchi, H. Masuda, Y. Tanigaki, and Y. Nojima, "Modified Distance Calculation in Generational Distance and Inverted Generational Distance," in *Evolutionary Multi-Criterion Optimization, 8th International Conference, EMO 2015*, A. Gaspar-Cunha, C. H. Antunes, and C. Coello Coello, Eds. Guimarães, Portugal: Springer. Lecture Notes in Computer Science Vol. 9019, March 29 - April 1 2015, pp. 110–125.

[18] O. Schütze, X. Esquivel, A. Lara, and C. A. Coello Coello, "Using the Averaged Hausdorff Distance as a Performance Measure in Evolutionary Multiobjective Optimization," *IEEE Transactions on Evolutionary Computation*, vol. 16, no. 4, pp. 504–522, August 2012.

[19] H. Ishibuchi, Y. Setoguchi, H. Masuda, and Y. Nojima, "Performance of Decomposition-Based Many-Objective Algorithms Strongly Depends on Pareto Front Shapes," *IEEE Transactions on Evolutionary Computation*, vol. 21, no. 2, pp. 169–190, April 2017.

[20] D. A. Van Veldhuizen, J. B. Zydallis, and G. B. Lamont, "Considerations in Engineering Parallel Multiobjective Evolutionary Algorithms," *IEEE Transactions on Evolutionary Computation*, vol. 7, no. 2, pp. 144–173, April 2003.

[21] D. A. V. Veldhuizen, "Multiobjective Evolutionary Algorithms: Classifications, Analyses, and New Innovations," Ph.D. dissertation, Department of Electrical and Computer Engineering. Graduate School of Engineering. Air Force Institute of Technology, Wright-Patterson AFB, Ohio, USA, May 1999.

[22] C. A. Coello Coello and N. Cruz Cortés, "An Approach to Solve Multiobjective Optimization Problems Based on an Artificial Immune System," in *First International Conference on Artificial Immune Systems (ICARIS'2002)*, J. Timmis and P. J. Bentley, Eds. University of Kent at Canterbury, UK, September 2002, pp. 212–221, iSBN 1-902671-32-5.

[23] K. Deb, A. Pratap, S. Agarwal, and T. Meyarivan, "A Fast and Elitist Multiobjective Genetic Algorithm: NSGA–II," *IEEE Transactions on Evolutionary Computation*, vol. 6, no. 2, pp. 182–197, April 2002.

[24] H. Ishibuchi, R. Imada, Y. Setoguchi, and Y. Nojima, "Reference Point Specification in Hypervolume Calculation for Fair Comparison and Efficient Search," in *2017 Genetic and Evolutionary Computation Conference (GECCO'2017)*. Berlin, Germany: ACM Press, July 15-19 2017, pp. 585–592, iSBN 978-1-4503-4920-8.

[25] M. T. Emmerich, A. H. Deutz, and I. Yevseyeva, "On reference point free weighted hypervolume indicators based on desirability functions and their probabilistic interpretation," *Procedia Technology*, vol. 16, pp. 532 – 541, 2014, cENTERIS 2014 - Conference on ENTERprise Information Systems / ProjMAN 2014 - International Conference on Project MANagement / HCIST 2014 - International Conference on Health and Social Care Information Systems and Technologies.

[26] R. Hernández-Gómez, C. A. C. Coello, and E. Alba, "A Parallel Version of SMS-EMOA for Many-Objective Optimization Problems," in *Parallel Problem Solving from Nature – PPSN XIV, 14th International Conference*, J. Handl, E. Hart, P. R. Lewis, M. López-Ibáñez, G. Ochoa, and B. Paechter, Eds. Edinburgh, UK: Springer. Lecture Notes in Computer Science Vol. 9921, September 17-21 2016, pp. 568–577, iSBN 978-3-319-45822-9.

[27] K. Deb, L. Thiele, M. Laumanns, and E. Zitzler, "Scalable Multi-Objective Optimization Test Problems," in *Congress on Evolutionary Computation (CEC'2002)*, vol. 1. Piscataway, New Jersey: IEEE Service Center, May 2002, pp. 825–830.

[28] S. Huband, P. Hingston, L. Barone, and L. While, "A Review of Multiobjective Test Problems and a Scalable Test Problem Toolkit," *IEEE Transactions on Evolutionary Computation*, vol. 10, no. 5, pp. 477–506, October 2006.

[29] M. T. Emmerich and A. H. Deutz, "Test Problems Based on Lamé Superspheres," in *Evolutionary Multi-Criterion Optimization, 4th International Conference, EMO 2007*, S. Obayashi, K. Deb, C. Poloni, T. Hiroyasu, and T. Murata, Eds. Matshushima, Japan: Springer. Lecture Notes in Computer Science Vol. 4403, March 2007, pp. 922–936.

[30] M. T. Emmerich, A. H. Deutz, and J. W. Kruisselbrink, "On Quality Indicators for Black-Box Level Set Approximation," in *EVOLVE - A bridge between Probability, Set Oriented Numerics and Evolutionary Computation*, E. Tantar, A.-A. Tantar, P. Bouvry, P. D. Moral, P. Legrand, C. A. Coello Coello, and O. Schütze, Eds. Heidelberg, Germany: Springer-Verlag. Studies in Computational Intelligence Vol. 447, 2013, ch. 4, pp. 157–185, 978-3-642-32725-4.